Xinjie. 2014. *Int. J. Vehicle Structures & Systems*, 6(3), 47-50
ISSN: 0975-3060 (Print), 0975-3540 (Online)
doi: 10.4273/ijvss.6.3.01

International Journal of Vehicle Structures & Systems
Available online at www.maftree.org/eja

Analysis of Plastic Oil-Gas Separator for Diesel Engine Valve Chamber Cover

Zhang Xinjie
Qingdao Agricultural University, Qingdao Shandong, China.
Email: zhxj200481@yahoo.com.cn

ABSTRACT:

Three different configurations of plastic oil-gas separator for diesel engine valve chamber cover were studied using numerical simulations. The distribution of flow velocity, pressure and oil droplets collection from simulation results were assessed to find out an optimum design for the oil-gas separator. Further, the oil-gas separation efficiency from simulation and experimental test was also reviewed to verify the simulation model as well as selection of the best design amongst the considered three configurations of the oil-gas separator.

KEYWORDS:

Diesel engine; Valve chamber; Oil-gas separator; Numerical simulation; Computational fluid dynamics

CITATION:

Z. Xinjie. 2014. Analysis of Plastic Oil-Gas Separator for Diesel Engine Valve Chamber Cover, *Int. J. Vehicle Structures & Systems*, 6(3), 47-50. doi:10.4273/ijvss.6.3.01.

1. Introduction

The emission of particles from the diesel engine crank case exhaust system is a concern for many vehicle manufacturers owing to tighter emission regulations. One way of tackling this issue is to improve the oil-gas separation efficiency. The existing diesel engine valve chamber cover and oil-gas separator are mostly aluminium casting, which leads to a heavy cover resulting in poor fuel economy. Plastic materials for valve chamber cover offer more complex oil-gas separator design to increase the oil-gas separation efficiency in diesel engines [1-2]. The oil-gas separator segregates the oil droplets from mixed gas through its internal partitions as shown in Fig. 1. The functioning of oil-gas separator involves complex three dimensional turbulence and two-phase flow. Hence, it is very difficult to predict the internal flow using analytical methods.

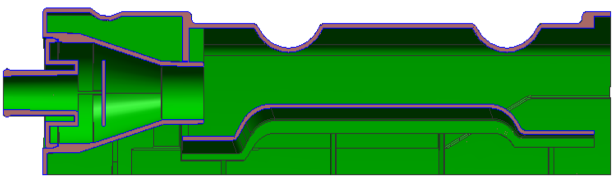

Fig. 1: Typical cross section of an oil-gas separator

Numerical simulation using computational fluid dynamics (CFD) benefits shorter time for product design and undertaking a complete analysis of the oil-gas separator with less capital investments. Hence, the fluid flow in the oil-gas separator investigation using numerical simulations is the main focus of this paper. Numerical simulations have been previously used in the literature for labyrinth oil-mist separator [3-6], gravity oil-gas separator [7-8] and cyclone oil-gas separator [9-10]. In this work, CFD simulations and experimental tests are undertaken to investigate the efficiency of sedimentation type separator with baffle (STB), labyrinth type separator with baffle (LTB) and labyrinth type (LT) separator. The flow velocity field, pressure field, oil droplets collection and oil-gas separation efficiency from the simulations were compared for the considered three designs to conclude an optimum structure for the oil-gas separator. The oil-gas separation efficiencies from simulations are also verified through laboratory experiments.

2. Simulation model and test bench

Discrete PHASE Model (DPM) is often used to model the simulation of gas-liquid two-phase flow. This model uses Eulerian equations to describe the gas phase flow field and Lagrange equations to describe the movement of oil droplets. In this paper, gas phase flow field is calculated using SIMPLE method. The trajectory of oil droplets is tracked using DPM. The force between gas flow and oil droplet in DPM is given by [11-12]:

$$F = \sum\left(F_D + F_Q\right) * m_S * \Delta t \tag{1}$$

Where m_S is oil droplet mass. F_Q force may include different forces, for example, gravity, buoyancy, pressure, temperature gradient force, Brownian movement force, false mass force, Basset force, Magnus force and Saffman force. F_D is gas flow resistance that is given by:

$$F_D = \frac{18\mu C_D Re}{24\rho_s d^2}\left(u_s - u\right) \tag{2}$$

Where u_s and u are liquid and gas phase velocity. d is oil droplet diameter. ρ_s and ρ_c are oil droplet and gas density. μ is dynamic viscosity. C_D is drag coefficient. Re is the relative Reynolds of oil droplet that is given by:

$$Re = \frac{\rho_c d}{\mu}\left|u_s - u\right| \tag{3}$$

The trajectory of oil droplet in gas flow can be derived from the oil droplet force. The momentum equation of oil droplets per unit mass is given by:

$$\frac{du_s}{dt} = -(F_D + F_Q) \tag{4}$$

Force of oil droplet and reaction force of gas is reversible. So a negative sign was added in the right hand side of Eqn. (4). In gas liquid two phase flow of separation, the diameter of oil droplets is very small and their concentration is very dilute. Hence, other forces can be neglected for being very small in magnitude compared to the fluid drag force.

Oil-gas separator geometric models of STB, LTB and LT designs are shown in Fig. 2 to Fig. 4. The oil-gas separator geometry is modelled using tetra elements with finite element size of 2mm. The simulation model generated using STAR CD version 3.2 software contains 587000 elements. The oil-gas separator material is PA66 + 15%Mineral + 25%GF with elastic modulus of 2084 MPa (150°C, RH0), Poisson's ratio of 0.33, density of 1470 kg/m^3, and coefficient of thermal expansion of 3.5×10^{-5} m/m/°C. Lagrangian multi-phase model with two phase flow respectively for air and oil droplet is used. Thermal modelling considers the effects of temperature change, heat transfer and thermal radiation. High Reynolds number turbulence is taken into account in the modelling. Gravity effects are considered in the simulation. Medium physical properties of oil and gas, as given in Table 1, are used for the simulation. Calculated fluid is assumed to be incompressible air. Piston air leakage of 180 *l*/min applied. The measured value of total oil droplet mass is 2 g/h before separation.

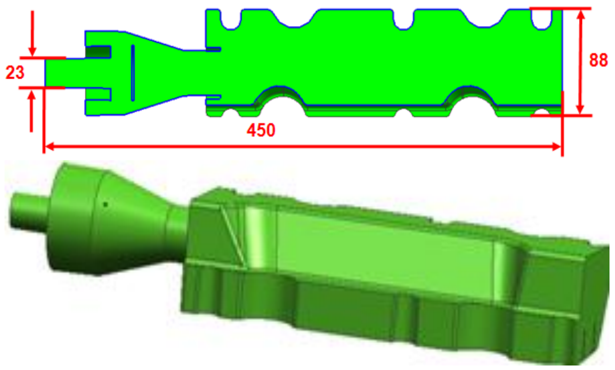

Fig. 2: Oil-gas separator – STB design

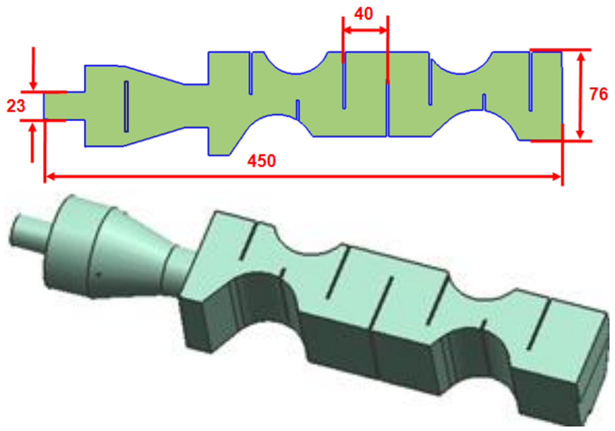

Fig. 3: Oil-gas separator – LTB design

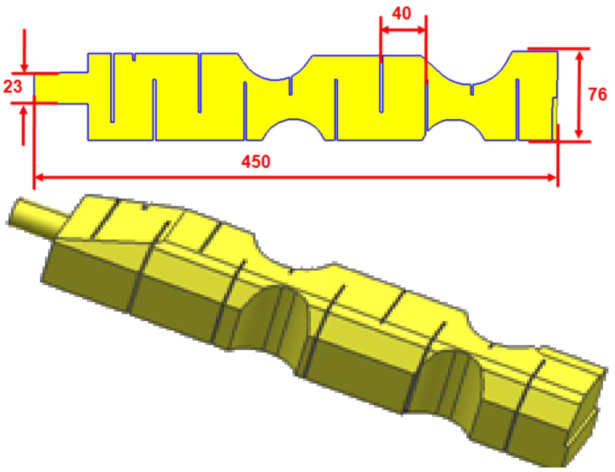

Fig. 4: Oil-gas separator – LT design

Table 1: Physical properties of oil and gas

Property	Fluid properties (Blow-by-gas)	Particle properties (Oil droplets)
Temperature	80°C	80°C
Density	1 kg/m³	843 kg/m³
Pressure	101325 Pa	-
Viscosity	2.09x10^{-5} Pa*s	-

The boundary layer was set as two layers. FAME grid was used. The grid was properly encrypted in the high velocity region. The model is analysed for steady state conditions. Simple algorithm is used for solving the CFD problem. Relaxation factor of all the calculated physical quantities is selected. Upwind difference scheme is used for distribution calculation.

3. Oil-gas separation efficiency

The oil-gas separation efficiency (η) is the ratio of the collected oil droplet mass (S_2) relative to the oil droplet mass entered (S_1) the cover per unit time and is given by:

$$\eta = \frac{S_2}{S_1} = \frac{S_1 - S_3}{S_1} = 1 - \frac{S_3}{S_1} \tag{5}$$

Where S_3 is oil droplet mass at outlet. The oil-gas separation efficiency is experimentally evaluated using a test bench as shown in Fig. 5. From the CFD simulation results, the oil-gas separation efficiency is calculated by:

$$\eta = \frac{N_1 - N_2}{N_1} = 1 - \frac{N_2}{N_1} \tag{6}$$

Where N_1 and N_2 are the unit number at inlet and outlet of the chamber cover respectively.

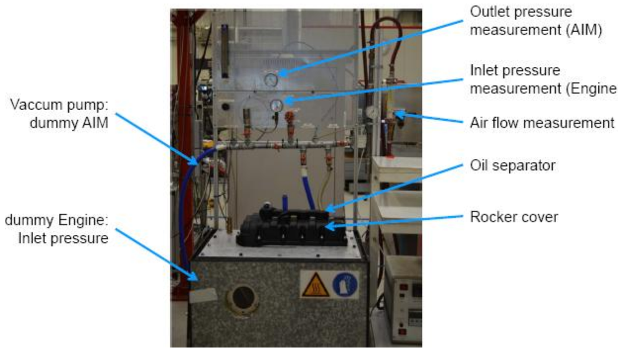

Fig. 5: Oil-gas separation efficiency test bench photograph

4. Results and discussions

The overall flow velocity, pressure distribution and pressure loss at inlet and outlet of the engine valve chamber cover are obtained from the gas continuous phase flow simulations. The flow velocity results of STB, LTB and LT oil-gas separator designs are shown in Fig. 6 to Fig. 8. Flow velocity of all designs at inlet is 0.6 m/s. For STB design, the flow velocity in sedimentation field was slow such that the oil droplet sinks easily into the separation chamber wall under its gravity and collection of oil droplets was completed. Flow velocity in the baffle field was fast such that the oil droplet was collected through fast impacts on baffle. For LTB design, mixed gases of oil and gas flow at higher speed in the labyrinth cavity and the oil droplet easily impacted the baffle. The mixed gas travelled along the S path in the cavity for easier collection of oil droplets. For LT design, the collection of oil droplets was completed by fast impact of oil droplets on labyrinth. The pressure distribution of STB, LTB and LT designs are shown in Fig. 9 to Fig. 11. A summary of peak velocity and pressure is given in Table 2. LT design proved to generate the fastest flow. STB design has the smallest pressure loss than the LTB and LT designs.

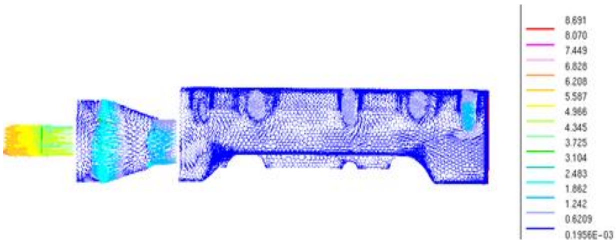

Fig. 6: STB design - Velocity (in m/s) distribution

Fig. 7: LTB design - Velocity (in m/s) distribution

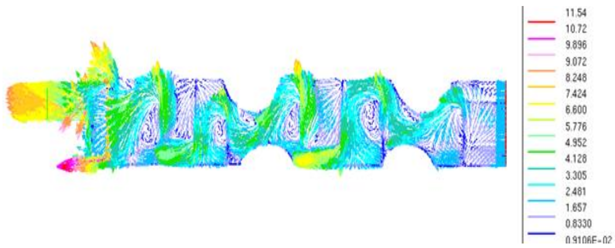

Fig. 8: LT design - Velocity (in m/s) distribution

Fig. 9: STB design - Pressure (in Pa) distribution

Fig. 10: LTB design - Pressure (in Pa) distribution

Fig. 11: LT design - Pressure (in Pa) distribution

Table 2: Comparison of peak velocity and pressure loss

Peak value	STB	LTB	LT
Velocity (m/s)	8.691	8.871	11.54
Pressure loss (Pa)	63.83	199.7	276.8

The distribution of oil droplet collection for STB, LTB and LT designs were in shown in Fig. 12 to Fig. 14. For STB design, much of oil droplet is collected in the sedimentation and baffle fields resulting in a more even distribution of droplet collection. LTB had much oil droplet collection in the baffle field. For LT design, oil droplets collection was mainly centralised in the labyrinth zone resulting in the best oil droplet collection amongst the considered three designs.

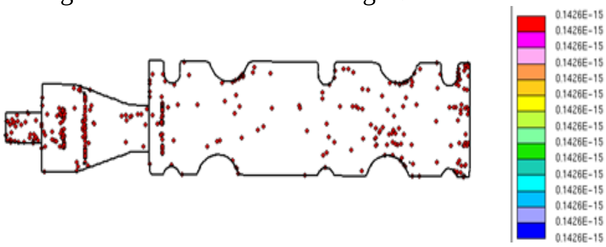

Fig. 12: Oil droplet capture (in kg) distribution of scheme one

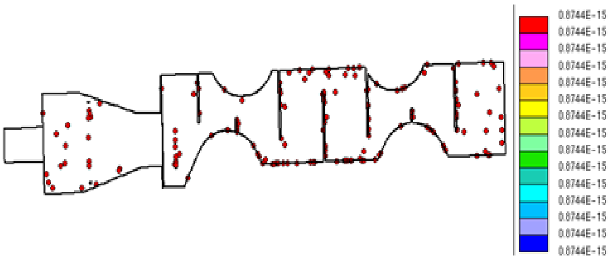

Fig. 13: Oil droplet capture (in kg) distribution of scheme two

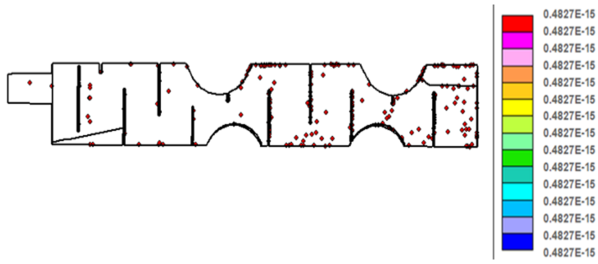

Fig. 14: Oil droplet capture (in kg) distribution of scheme three

The oil-gas separation efficiencies from numerical simulations and experimental tests for STB, LTB and LT designs of oil-gas separator are shown in Table 3. The efficiency results from tests are better than the simulation ones. The test separation efficiency of LT design was the best one when compared with the efficiencies of STB and LTB designs. Hence, LT design was adopted as an optimum design for the oil-gas separator of the diesel engine valve chamber cover.

Table 3: Oil-gas separation efficiency – Simulation vs. Test

Diameter (μm)	Simulation results (%)			Test results (%)		
	STB	LTB	LT	STB	LTB	LT
3	65	67	68	67	68	70
5	67	68	72	70	72	75
10	72	74	79	76	78	85

5. Conclusions

Numerical simulation of oil-gas separator for diesel engine valve chamber cover was carried out using CFD software. Gas phase flow field, oil droplet motion and oil-gas separation efficiency were analysed for STB, LTB and LT design configurations of oil-gas separator. Experimental tests were carried out to predict the oil-gas separation efficiency. Based on the results from simulations and tests, the labyrinth type configuration was found to be an optimum design for the oil-gas separator amongst the considered three configurations. The separation efficiencies from simulation were lesser than those from the experimental tests. This may be due to the negligence of oil droplet rebound motion.

REFERENCES:

[1] F. Meibin. 2009. Development and applications of new materials in automotive light weighting technologies, *Automobile Technology & Materials*, 2, 6-9.

[2] F. Zijie, G. Liangjin and S. Ruiyi. 2014. Research and development of automotive light weight technology, *J. Automotive Safety and Energy*, 1, 1-16.

[3] T. Lifang, W. Cheng, L. Rong, X. Yafei and Y. Wenle. 2010. CFD analysis for the separation efficiency of a labyrinth oil mist separator, *Diesel Engine*, 32(5), 19-22.

[4] S. Xiujun, S. Haiou and J. Renqiu. 2006. Numerical simulation of locus of oil droplet in oil air separator, *Applied Science and Technology*, 33(10), 69-72.

[5] F. Jianmei, C. Yunfeng, Q. Zongchang and Y. Jianguo. 2006. Numerical simulation of oil droplets traces in oil gas separator, *J. Xian Jiaotong Univ.*, 40(7), 771-775.

[6] D.G. Zhian, J. Lin, S. Jie and D. Xin. 2010. Numerical simulation of the flow field inside the oil gas separators with different regulating components, *J. Xi'an Shiyou University*, 25(4), 32-35.

[7] H. Jingyan, S. Sheng, W. Fengkai and H. Jin. 2013. Simulation analysis and test verification on oil-gas separator of gasoline direct injection engine, *Computer Aided Engg.*, 2(5), 11-15.

[8] S. Xiujun, S. Haiou and J. Renqiu. 2013. Numerical simulation of the flow field around coalescing element separation in gravity oil-gas separator, *Guangdong Chemical Industry*, 40(2), 124-125.

[9] G. Guang-dong, D. Song-sheng, H. Wei-xing and Z. Xing-gang. 2013. Numerical simulation of oil droplets motion trajectory within dynamic liquid-liquid hydrocyclone, *J. Logistical Engg. Univ.*, 29(3), 24-29.

[10] J. Feng, X. Yang, X. Gao and Y. Chang. 2011. Numerical simulation and experiment on oil gas cyclone separator, *J. Xi'an Jiaotong University*, 45(7), 55-59.

[11] W. Weishu, X. Weihui, Z. Zhao-jiang, M. Qingdong, C. Tingkuan and L. Yu-shan. 2007. Realization of PISO algorithm and comparison convergence characteristics with simple series algorithms, *J. North China Inst. Water Conservancy & Hydroelectric Power*, 31(3), 51-55.

[12] C. Xiao-hua and L. Chun-guang. 2011. Application and Study of Simplec Algorithm with Colocated Grides, *J. Gansu Lianhe University*, 25(3), 40-44.